Upper crust reworking during gravitational collapse: the Bembibre–Pico Sacro detachment system (NW Iberia)

JUAN GÓMEZ BARREIRO[1]*, JOSÉ R. MARTÍNEZ CATALÁN[2], RUBÉN DÍEZ FERNÁNDEZ[2], RICARDO ARENAS[1] & FLORENTINO DÍAZ GARCÍA[3]†

[1]*Departamento de Petrología y Geoquímica–Instituto de Geología Económica CSIC, Universidad Complutense, 28040, Madrid, Spain*

[2]*Departamento de Geología, Universidad de Salamanca, 37008 Salamanca, Spain*

[3]*Departamento de Geología, Universidad de Oviedo, 33005 Oviedo, Spain*

†*Deceased*

**Corresponding author (e-mail: jugb@usal.es)*

Abstract: The kinematics of the basal allochthon in the SW of the Órdenes Complex is analysed to constraint its evolution during collisional and postcollisional stages of the Variscan orogeny. Two distinct sequences have been identified in the basal allochthon of this sector: the upper and lower sequences, in close correlation with the subdivision of the basal allochthon in the Malpica–Tui Complex. Three main tectonic episodes have been established in the basal allochthon: a high-pressure event related to continental subduction, a mesozonal event of regional exhumation by thrusting and recumbent folding, and a regional-scale extensional episode that resulted in the development of the Bembibre–Pico Sacro detachment system. The Bembibre–Pico Sacro system rejuvenated pre-existing shear zones, whose weakness favoured the nucleation of the detachments. Shear zones associated with the detachments overprinted the previous tectonic fabrics under conditions ranging from lower amphibolite to greenschist facies, and with heterogeneously distributed ductile to brittle deformation. The detachment system is coeval with late orogenic collapse and widespread magmatism, and represents its upper crustal expression. It correlates with mid- and lower crustal flow and the development of gneiss domes at depth in such a way that the basal allochthon can be considered a rheological boundary between the more rigid allochthonous sequences above and the more viscous Schistose Domain and autochthon below.

Continental lithosphere is characterized by cumulative growth during orogenic periods. Long-term persistence of the structural architecture, particularly shear zones and faults, and the overlapping of fabrics, metamorphic events and magmatic episodes, determines the way in which the lithosphere reacts to every new tectonothermal event (Neil & Houseman 1997; Holdsworth *et al.* 2001; Houseman & Molnar 2001). The existence of mechanical discontinuities and the variation of lithospheric thermal state seem to be essential controls that potentially shape subsequent episodes (Butler *et al.* 1997; Holdsworth *et al.* 1997). Regional studies in collisional scenarios on tectonic renewal of both discrete structures (reactivation) and, at a larger scale, lithospheric or crustal volumes (reworking) are critical to understanding the rheological behaviour of an orogenic belt with time.

In this context, the geodynamic evolution of the basal allochthon in the NW Iberian Massif is examined. The basal allochthonous units are key pieces of the intricate and long-standing Variscan orogenic puzzle. They represent the outermost edge of the Gondwana supercontinent, having undergone distinct tectonothermal events related to the continental subduction (D_1) and subsequent collisional deformation (D_2) during the Variscan orogeny. However, their role during late orogenic extensional collapse (D_3) remains obscure. Here we focus on this third event (D_3), during which regional-scale extensional detachments partially rejuvenated previous structures and dominated the deformation of the basal allochthon.

Geological context

The NW Iberian Massif includes an autochthonous realm formed by metamorphic rocks ranging from very low grade to catazonal, and by plutonic rocks. Allochthonous units occur above the Iberian autochthon, and represent the remnants of a huge and structurally complex nappe stack formed by terranes with different degrees of exoticism. Among the five existing allochthonous complexes, Cabo Ortegal, Órdenes, Malpica Tui, in Spain, and Morais and Bragnaça, in Portugal, the Órdenes Complex is the largest (Fig. 1; Martínez Catalán *et al.* 2009) and includes the full sequence of allochthonous units recognized.

The allochthonous units are grouped according to their origin and the structural position they occupy in the nappe pile. They include pieces of a Cambro-Ordovician ensialic island arc on top (upper allochthon, Andonaegui *et al.* 2002; Santos *et al.* 2002; Abati *et al.* 2003; Castiñeiras 2005; Gómez Barreiro *et al.* 2006; Castiñeiras *et al.* 2010), and distal parts of the Gondwanan continental margin at the bottom (basal allochthon, Martínez Catalán *et al.* 1996). Sandwiched in an intermediate structural position, several ophiolitic units appear, including relicts of a Cambro-Ordovician back-arc (Arenas *et al.* 2007; Sánchez Martínez *et al.* 2007*a*), a possible record of Ordovician oceanic crust (Pin *et al.* 2006), and Early Middle Devonian suprasubduction-zone type ophiolites (Díaz García *et al.* 1999; Pin *et al.* 2002, 2006; Sánchez Martínez *et al.* 2007*b*; Gómez Barreiro *et al.* 2010).

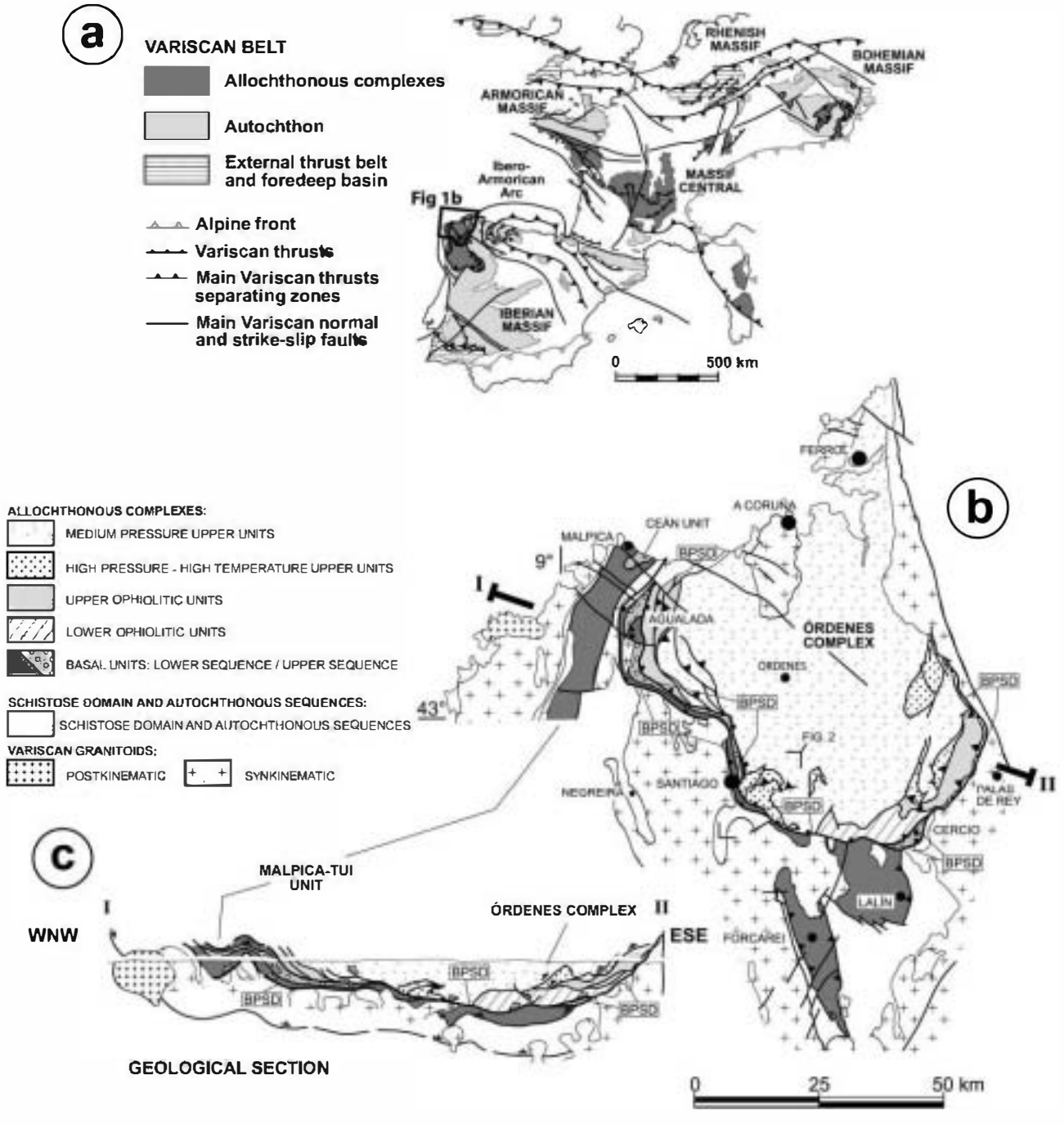

Fig. 1. (a) Location of the study area in the Variscan belt of Europe; (b) map showing the allochthonous complexes of Órdenes and northern half of Malpica–Tui in Galicia, NW Spain; (c) a representative cross-section showing the general structure. The nappe stacking and the position of the lower and upper sequences within the basal allochthon should be noted. Top-to-the-ESE kinematics often represents thrusting, whereas top-to-the-WNW kinematics is related to extensional collapse and reactivation of previous structures. BPSD, Bembibre–Pico Sacro detachment system. The location of Figure 2 is indicated. After Gómez Barreiro *et al.* (2007) and Díez Fernández *et al.* (2010).

The stacking order of the allochthonous units reproduces the evolving palaeogeographical scenario in the northern Gondwanan margin. This includes the development and drifting away of an ensialic island arc (upper allochthon) leaving behind a long history of crustal extension in Gondwana (Abati *et al.* 2010), which culminated with the birth and spreading of the Rheic Ocean (ophiolitic allochthon). The closure of this oceanic realm marked the beginning of the assembly of Pangaea (Gómez Barreiro *et al.* 2010), which started in the European Variscides with the subduction of the outermost continental margin of Gondwana, represented by the basal allochthon in the NW Iberian Massif.

Below the allochthonous units, an imbricate thrust sheet separates the basal, ophiolitic and upper units from the autochthon. It consists of Ordovician and Silurian metasediments and volcanic rocks (Farias *et al.* 1987; Rodríguez *et al.* 2004; Valverde-Vaquero *et al.* 2005), and is known as the parautochthon (Ribeiro *et al.* 1990), the Schistose Domain (Farias *et al.* 1987), or the lower allochthon (Martínez Catalán *et al.* 2009). No ophiolites have been found either inside this sequence or at its base, and it is considered a relatively distal part of the Gondwanan continental margin, less distal than the basal allochthon, which underwent early Variscan subduction whereas the Schistose Domain did not.

This study is focused on the basal allochthon in the southwestern part of the Órdenes Complex. In this area the basal allochthon consists of terrigenous metasediments and igneous rocks, traditionally grouped under the local name of Santiago unit (Martínez Catalán *et al.* 1997; Figs 1 and 2), tracing the general structure along the western limb of the Órdenes Complex. The upper allochthon on top (Fig. 1) is represented by the intermediate-*P* schists and paragneisses of the O Pino unit (Figs 1 and 2), and the high-*P* and high-*T* metabasites of the Fornás unit (Figs 1 and 2). Evidence discussed below suggests that the ophiolitic allochthon was tectonically removed in this sector (Fig. 1). The Schistose Domain schists in this part appear partially melted and intruded by granitoids (Fig. 1).

The basal allochthon in the SW of the Órdenes Complex

It has been recently recognized that the basal allochthon comprises two tectonically juxtaposed metasedimentary sequences, the upper and lower sequences (Fig. 1; Díez Fernández *et al.* 2010). Both of them underwent an initial high-*P* metamorphic event (D_1), their *P*–*T* conditions varying according to their primary location in a crustal subduction complex. The upper sequence reached blueschist-facies conditions (Arenas *et al.* 1995; Rodríguez *et al.* 2003; López Carmona *et al.* 2010) whereas the lower sequence developed eclogite-facies meta-

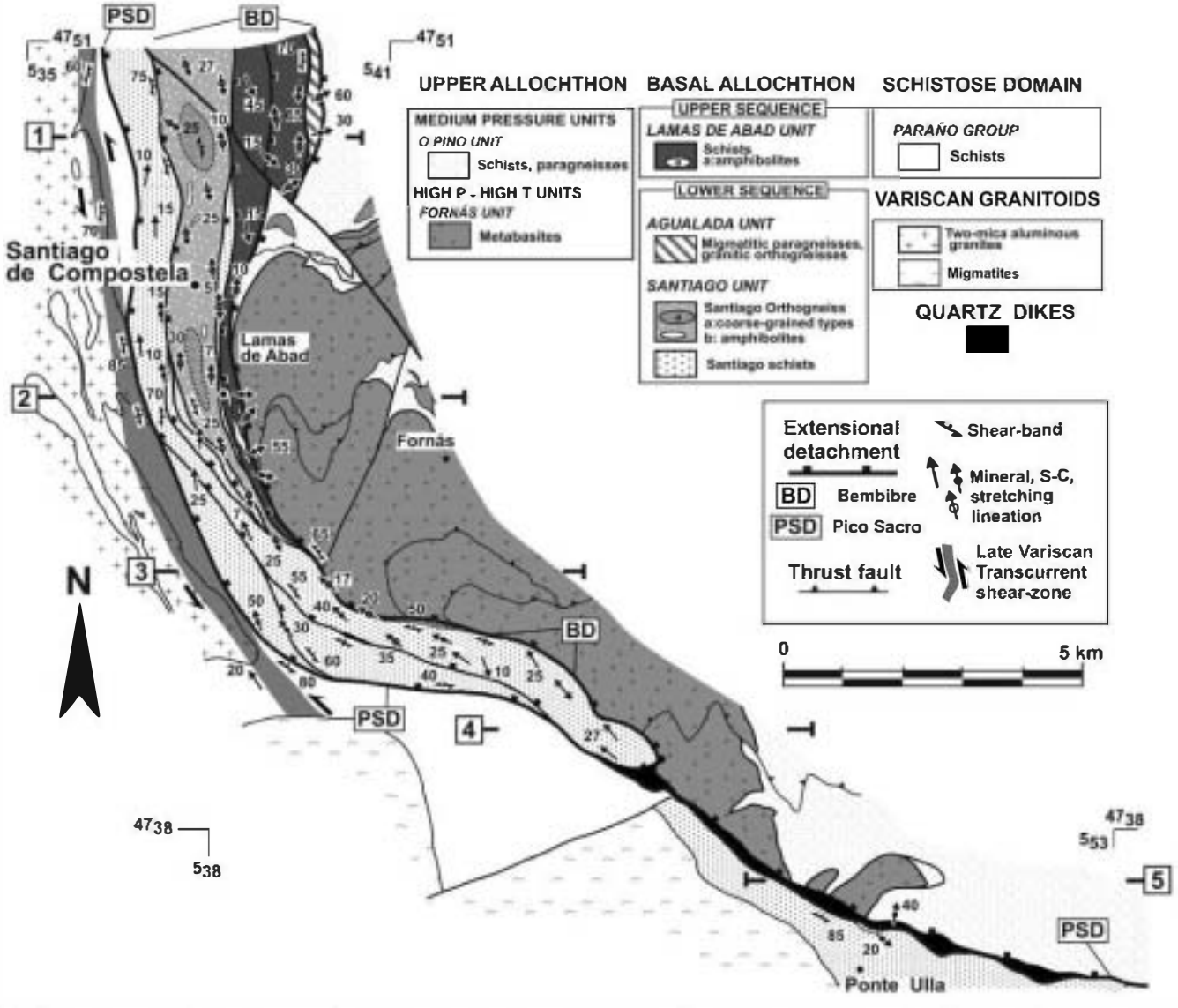

Fig. 2. Geological map of the SW of the Órdenes Complex. Location of cross-sections 1–5 of Figure 4 is shown. PSD, Pico Sacro detachment; BD, Bembibre detachment. Lineations and shear bands within the basal allochthon are indicated.

morphism (Gil Ibarguchi & Ortega Gironés 1985; Arenas *et al.* 1997; Rubio Pascual *et al.* 2002; Rodríguez *et al.* 2003). Based on the lithological association and tectonometamorphic evolution, the Agualada, Santiago, Lalín and Forcarei units belong to the lower sequence. However, new evidence described in detail below demonstrates that the upper half of the Santiago unit should be considered a distinct assemblage, belonging to the upper sequence (Fig. 1). The Cercio unit, composed of an alternation of micaschists and amphibolite lenses, may be included in the upper sequence, although no traces of a high-*P* event have been found.

A second tectonothermal episode (D_2) later affected the upper and lower sequences. It is related to the exhumation of the units through a combination of recumbent folding and thrusting with a general top-to-the east movement (Martínez Catalán *et al.* 2002). Differences exist here as a result of the formation of an inverted metamorphic zoning, from high-*T* amphibolite-facies conditions at the top to low-*T* amphibolite- to greenschist-facies conditions below. This event is related to the thrusting of lower sequence units (e.g. Agualada unit) over upper sequence ones (Fig. 1; Arenas *et al.* 1995; Rubio Pascual *et al.* 2002; Gómez Barreiro 2007).

A third event (D_3) may be identified, which is closely related to late orogenic readjustments. Regional-scale extensional detachments, north south upright folding and strike-slip shear zones heterogeneously overprint and rejuvenate the previous tectonometamorphic architecture, mostly under low-grade conditions (Gómez Barreiro *et al.* 2007). This is the episode that will be explored in detail below.

Tectonometamorphic units

A detailed analysis has been carried out on the SW branch of the basal allochthon, in the Órdenes Complex, where a continuous section crops out from the upper allochthon at the top to the Schistose Domain at the bottom (Figs 2 4). The geological cross-section reveals a complex distribution of shear zones and retrogression, resulting in structural mixing of several lithotypes and tectonothermal events. The basal allochthon in the SW of the Órdenes Complex has been traditionally considered to be represented by the Santiago unit (Arenas *et al.* 1995; Rubio Pascual *et al.* 2002; Martínez Catalán *et al.* 2009), but evidence presented below suggests that the boundaries of the Santiago unit should be revised, and that more tectonometamorphic units are involved. The units recognized at present are described below in structural order from top to bottom (east to west geographically; Fig. 4).

Agualada unit. This unit here is composed of well-preserved metre- to kilometre-sized lenses of migmatitic paragneisses and granitic orthogneisses (Figs 5, 6a and b). The migmatitic paragneisses, which are semipelitic in origin, show a strong schistosity defined by muscovite, which is progressively replaced by biotite. Plagioclase and quartz are recrystallized in a mosaic texture. Small idiomorphic garnets appear included within plagioclase and biotite crystals. White mica aggregates and small needles of aluminosilicates are also found. The paragneisses are spatially linked to leucocratic melts, which are made up of plagioclase, quartz, biotite and garnet. Rutile is preserved within garnet, whereas ilmenite is the Ti-phase in the matrix. Spatial relationships and mineralogy suggest a migmatitic origin. Small to medium grain-size granitic orthogneisses are locally preserved. Their mineral composition includes quartz, K-feldspar (microcline), biotite and garnet.

The lithological and mineral assemblage indicates a higher metamorphic grade than in the underlying schists, being compatible with high-temperature amphibolite-facies conditions. Given the equivalent structural position within the basal allochthon and

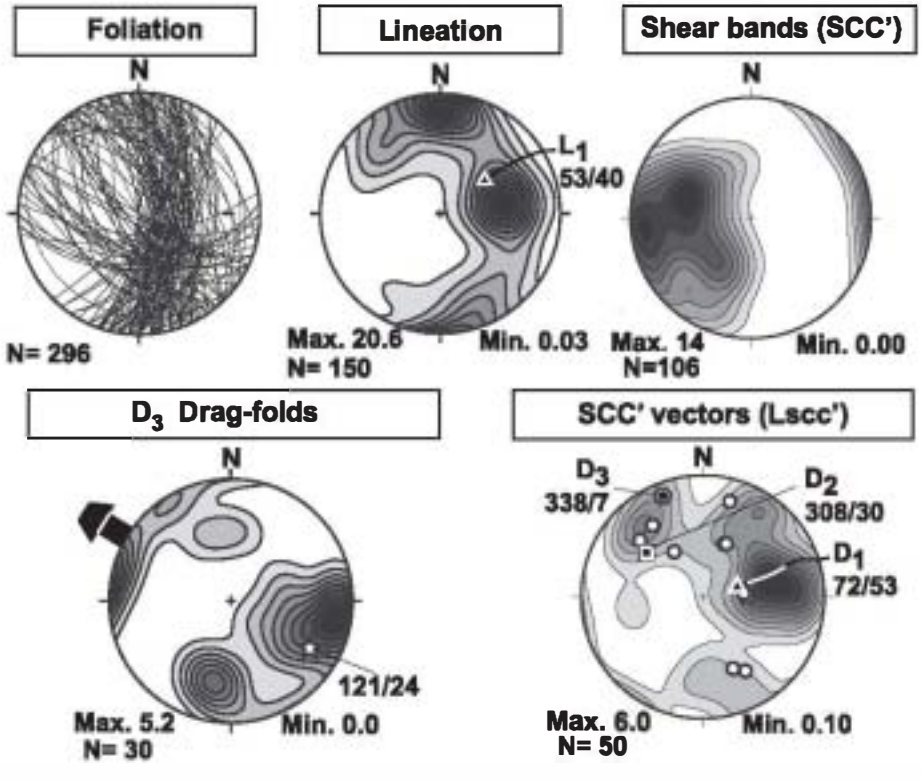

Fig. 3. Structural features of the SW of the Órdenes Complex summarized in stereograms. The foliation, lineation and shear bands (SCC') are shown for units of the basal allochthon. $L_{SCC'}$ vectors for D_1, D_2 and D_3 are indicated. Open circles represent distinct directional groups of D_3 $L_{SCC'}$ vectors. The movement direction derived from axes of D_3 drag folds associated with the hanging wall of the Bembibre–Pico Sacro detachment is also plotted. Lower hemisphere projection.

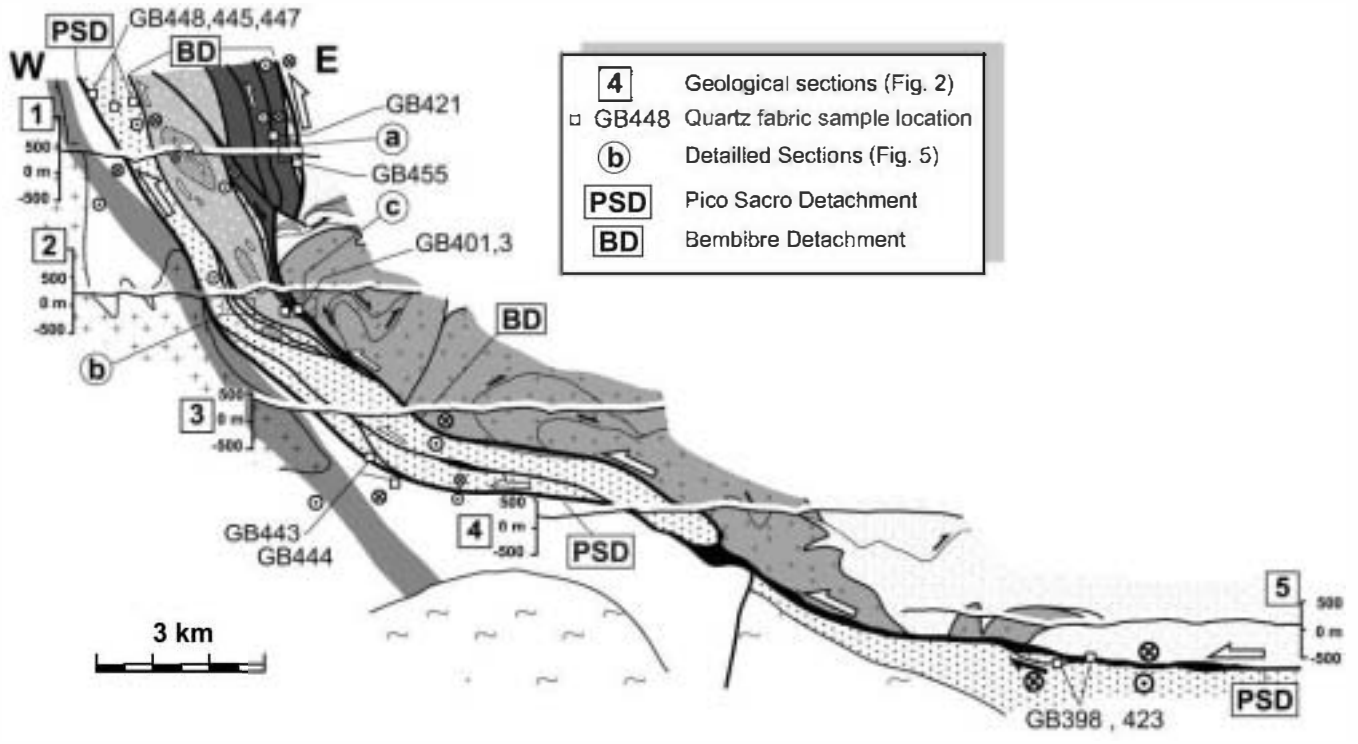

Fig. 4. Composite geological cross-section of the SW of the Órdenes Complex. The location of cross-sections 1–5 is indicated in Figure 2. Location of cross-sections a, b and c for Figure 5 is shown. The sample locations for quartz universal-stage crystallographic analysis are indicated (Fig. 9).

petrological similarities, these migmatitic gneisses represent here the southern prolongation of the Agualada unit, which belongs to the lower sequence units (Fig. 1), occupying an equivalent structural position within the basal allochthon. There, P–T estimations from eclogitic lenses yielded conditions of 15 kbar and 720 °C (Arenas *et al.* 1997). Although no eclogites have been found to date in our study area, petrological evidence suggests a linkage between the two segments of the basal allochthon. Moreover, late retrogression here is more intense than in the Agualada unit to the north, and should have had the effect of blurring the metamorphic record.

The orthogneisses locally developed an SC fabric (Berthé *et al.* 1979; Lister & Snoke 1984), with a general top-to-the-west sense of shear. Within C-planes, retrogression is marked by the presence of chlorite, white mica and minor epidote, suggesting greenschist-facies conditions (D_3). This fabric evolves across a gradient towards true phyllonites outside the orthogneisses, leading to a complete retrogression of the primary assemblages, where a mixture of chlorite, quartz and white mica defines a new fabric (S_3; Fig. 7c).

Lamas de Abad unit. Underlying the Agualada unit a strongly mylonitized schistose unit occurs, with a penetrative mylonitic foliation marked by quartz ribbons and mineral shape orientation (Figs 6c, d and 7a). Lenses of metabasites with hornblende, plagioclase, zoisite, titanite, rutile and chlorite are intercalated with the metasediments. Veins of plagioclase, quartz and zoisite are locally abundant in close relation to shear zones. Pelitic to semipelitic micaschists show a main fabric that includes coarse garnet and plagioclase porphyroblasts (maximum 6–8 mm), white mica, quartz, biotite, rutile, ilmenite, chlorite, epidote and clinozoisite. Plagioclase appears preferentially concentrated in layers. Interestingly, garnet shows two distinct textural positions: (1) micaceous domains, in which small and idiomorphic garnet grains grow in equilibrium with white mica; these domains appear bounded by late C' shear bands, with a top-to-the-NW sense of shear, in which a greenschist-facies mineral association develops (D_3; Fig. 6c); (2) large syntectonic porphyroblasts displaying an internal foliation (S_i) roughly defined by rutile and opaque minerals. The internal foliation shows continuity with the external foliation and, in some cases, snowball geometry. Garnet porphyroblasts develop σ and δ types within most deformed levels, which is in accordance with a general top-to-the-east SCC' fabric (Figs 6d and 7g, i).

Taking into account all these features and its structural position, the Lamas de Abad unit can be tentatively correlated with other units of the upper sequence in the basal allochthon. To the west, in the Ceán unit, whose mineral assemblages indicate equilibrium under blueschist-facies conditions, the schists display similar mineral assemblages and textural relationships, whereas the metabasites show conspicuous lawsonite pseudomorphs, and retrogression through amphibolite and greenschist facies (Gil Ibarguchi & Ortega Girones 1985; Rodríguez Aller 2005; López Carmona *et al.* 2010). To the east, the Cercio unit occupies an equivalent structural position and shows a similar lithological association, but absence of high-P event. Similarities as well as differences suggest that the Lamas de Abad unit represents the same tectonostratigraphic sheet as the Ceán and Cercio units, and occupied an intermediate position between them in an east–west-oriented strike section (Fig. 1).

Santiago unit. This unit consists of two main lithologies: Santiago schists below and Santiago orthogneiss above. A narrow band of Santiago schists also occurs between the Lamas de Abad unit and the Santiago orthogneiss, close to the city of Santiago de Compostela (Figs 2, 4 and 5), but to the north the Lamas de Abad unit appears in contact with the Santiago orthogneiss. This supports a subtractive character for the contact, suggested by the

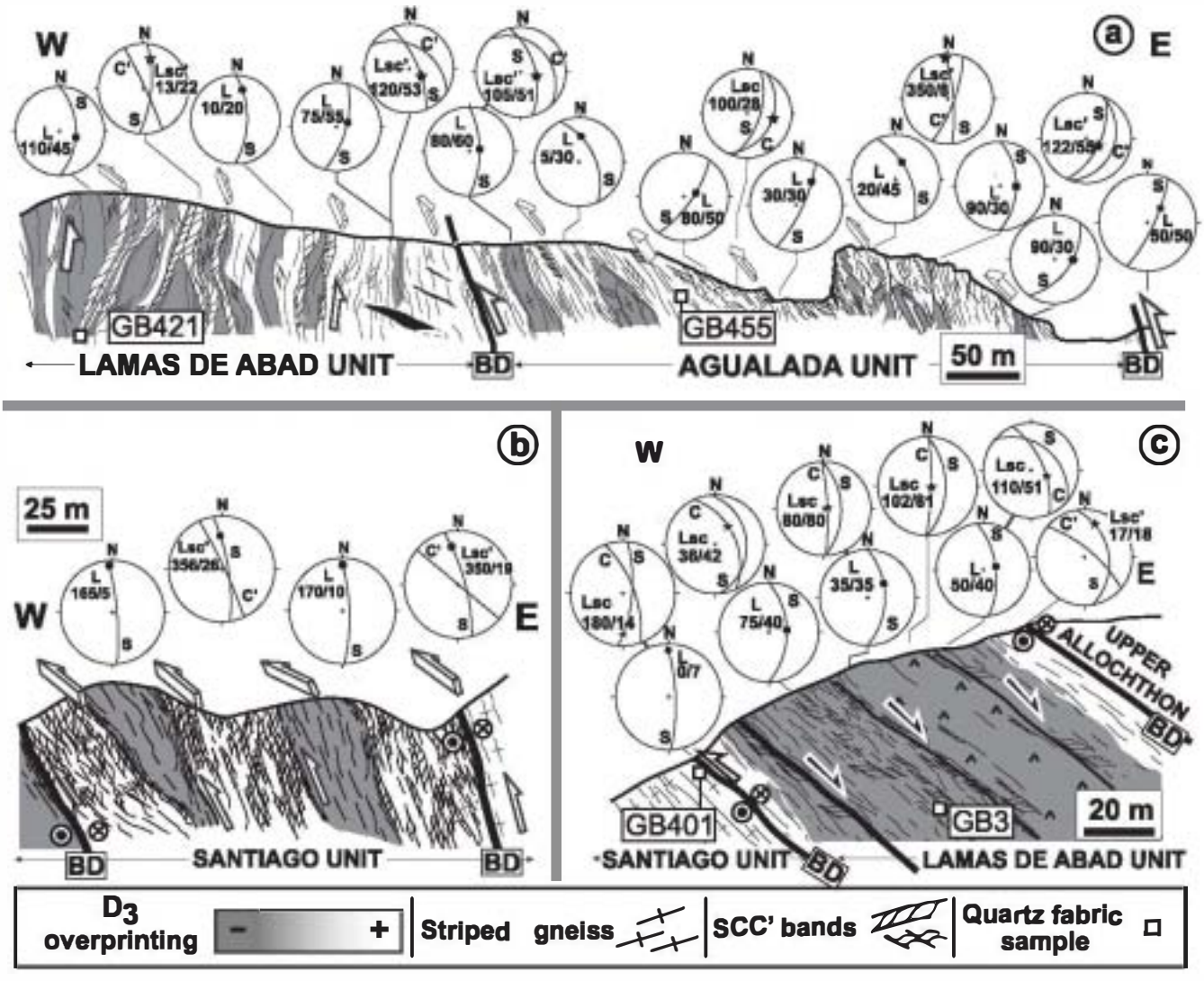

Fig. 5. Representative field geological sections of the Bembibre detachment shear zone. D_3 overprinting is indicated; dark grey indicates no D_3 overprinting. Shape (L and S) and SCC' fabric orientations are represented in equal angle, lower hemisphere stereograms. (**a**) Tectonic transition from the upper allochthon to the top of the basal allochthon, and the contact between the Agualada and Lamas de Abad units. A phyllonitic network was developed in both units. (**b**) Condensed transition from the upper allochthon to the Santiago orthogneiss. The Lamas de Abad unit shows a consistent top-to-the-ENE kinematics. (**c**) Lower contact of the Santiago orthogneiss with the Santiago schists. Striped gneisses appear in contact with phyllonites, with a consistent top-to-the-NNW sense of shear. The location of samples of Figure 9 is indicated.

fact that metasedimentary sequences above and below the granitic gneisses differ not only in composition but also in their metamorphic evolution. It also suggests a tabular shape for the orthogneiss before the development of the contact, because its upper and lower boundaries are parallel. The parallelization was acquired during ductile deformation associated with both subduction and exhumation by recumbent folding and thrusting (Díez Fernández & Martínez Catalán 2009). However, the orientation of the tectonic upper contact, parallel to the bottom of the orthogneiss, suggests a reactivation of the lithological contact.

Santiago schists. This is the most common lithology below the Lamas de Abad unit. The schists are semipelitic metasediments with distinct syntectonic albite porphyroblasts, which appear elongated parallel to and marking a mineral lineation. The schists are heterogeneously phyllonitized and retrogressed, especially in the vicinity of the main contacts (Fig. 6e). Mineral inclusions within albite porphyroblasts define an internal foliation ($S_i = S_1$) that has been barely transposed, representing a relic of a high-pressure low-temperature assemblage (D_1; Arenas *et al.* 1995).

Differences in mineral composition exist within the schists above and below the Santiago orthogneiss. Schists above show an S_2 foliation defined by biotite, white mica, quartz, plagioclase and chlorite, with minor ilmenite, titanite and garnet. Within albite porphyroblasts, the grain-size range of inclusions defining S_i is 50–200 μm. S_i is defined by small garnets and oriented crystals of white mica, epidote, rutile or ilmenite, chlorite and quartz. White mica (WM, Fig. 6e) has been identified as phengite (Arenas *et al.* 1995). This mineral assemblage can be correlated with a low-T eclogitic event related to the subduction of the basal allochthon (D_1). Below the orthogneiss, the main fabric (D_2) is defined by white mica, chlorite, plagioclase, quartz, ilmenite and titanite. Mineral inclusions in albite are very small (<10 μm),

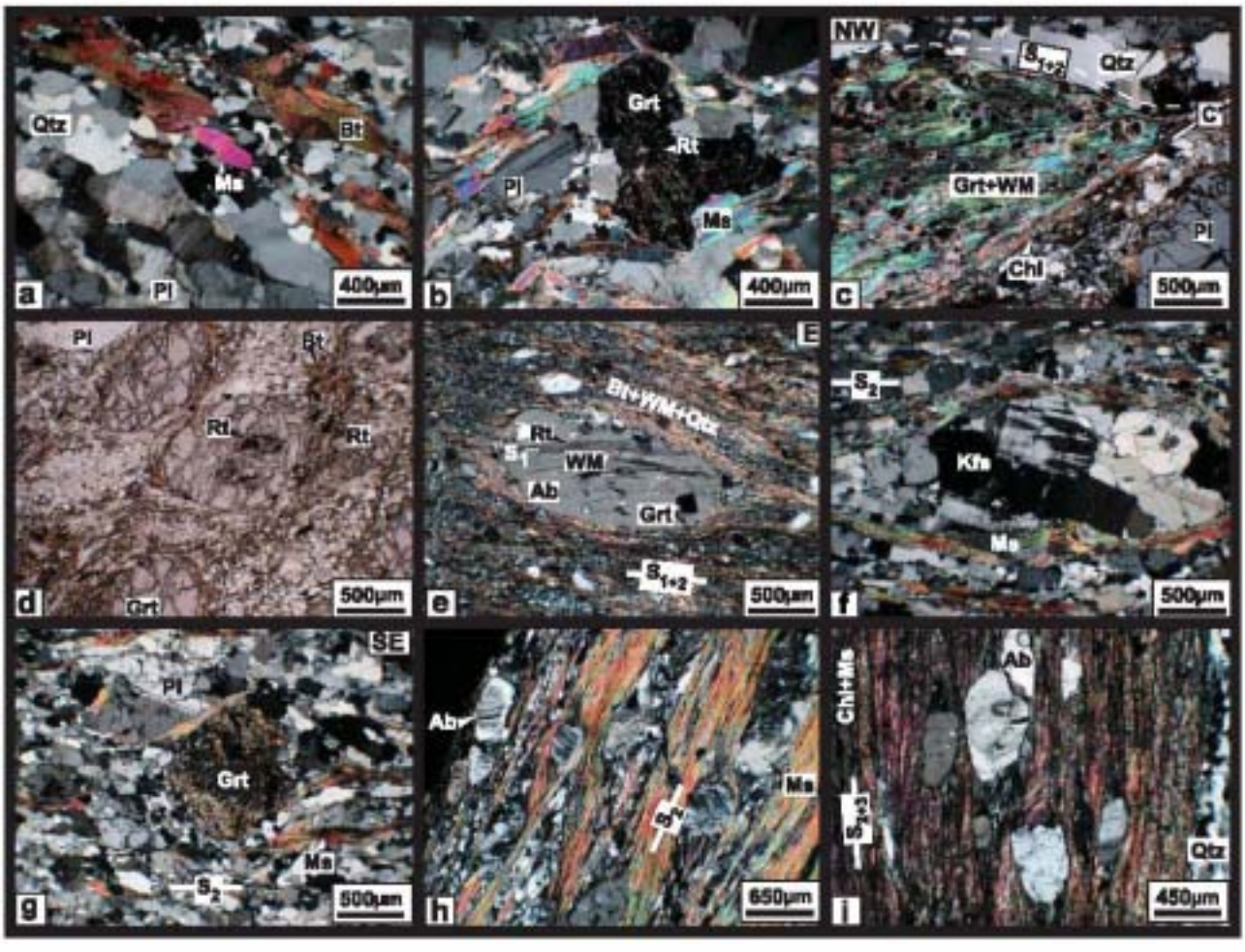

Fig. 6. Microstructural features of the basal allochthon in the SW Órdenes Complex. (a, b) Migmatitic paragneisses of the Agualada unit. (c, d) Lamas de Abad unit with high-*P* assemblages preserved. (e) Upper slice of Santiago schists, with albite (syn-D_2) porphyroblast. (f, g) Coarse-grained facies of the Santiago orthogneiss, where the mylonitic foliation defined by muscovite (S_2) surrounds igneous K-feldspar porphyroclasts (Kfs; f), and garnet (Grt; g). (h, i) Lower slice of the Santiago schists, where albite porphyroblasts show a very fine S_i with rutile (Rt), carbonaceous inclusions and epidote. The main foliation is defined by muscovite (Ms), chlorite (Chl) and quartz (Qtz).

defining an $S_i = S_1$ foliation by a mixture of carbonaceous inclusions, white mica, rutile or ilmenite needles, quartz and probably epidote (Fig. 6h and i). Differences in S_1 grain size and mineral assemblages suggest that the schists below the Santiago orthogneiss reached lower-grade conditions during D_1 metamorphic peak. Furthermore, differences found in the regional foliation (S_2) show that the upper schists reached the biotite zone, whereas the lower schists never exceeded the chlorite zone (Gómez Barreiro 2007), which supports the metamorphic inversion identified to the north by Arenas *et al.* (1995).

It should be noted that the regional foliation (D_2) at the bottom of the Santiago unit was locally overprinted by andalusite- and (locally) sillimanite-bearing assemblages, composed of muscovite, plagioclase, aluminosilicate, chlorite, quartz and biotite, which correlate with incipient partial melting at deeper levels in the Santiago schists cropping out to the south of the area (Figs 2 and 7b). Rotated andalusite porphyroblasts indicate synkinematic growth during top-to-the-north shearing. Low-*P* and intermediate- to high-*T* conditions have been suggested for this localized event (D_3; Gómez Barreiro 2007).

Santiago orthogneiss. Granitic gneisses cropping out as a tabular body (Figs 1, 2 and 4) divide the Santiago unit into two tectonic slices. Their thickness is drastically reduced from roughly 1 km to less than 50 m in the southern part of the area. The orthogneiss shows a mylonitic foliation with quartz, K-feldspar (microcline), white mica and garnet. Other phases include chlorite, apatite, epidote, biotite and ilmenite or titanite (Díaz García 1990; Gómez Barreiro 2007). The plutonic origin of the orthogneiss is deduced from textural criteria (Díaz García 1990). Coarse fabrics dominate the inner parts of the massif (Figs 6f, g and 8), with a gradual transition towards striped gneisses with a strong mylonitic foliation close to the boundaries (Fig. 7e). Amphibolite lenses, probably representing mafic dykes, have been identified (Fig. 2), whereas similar rocks to the north preserve eclogitic assemblages (Rubio Pascual *et al.* 2002).

Lithological association and metamorphic evolution correlate with lower sequence units in the basal allochthon to the west (Fig. 1; Malpica–Tui complex; Rodríguez Aller 2005; Díez Fernández *et al.* 2010). Mineral assemblages and regional evidence suggest that after the eclogite-facies event (D_1), mylonitic fabric re-equilibrated under amphibolite-facies conditions (D_2; Rubio Pascual *et al.* 2002). It has been argued that the

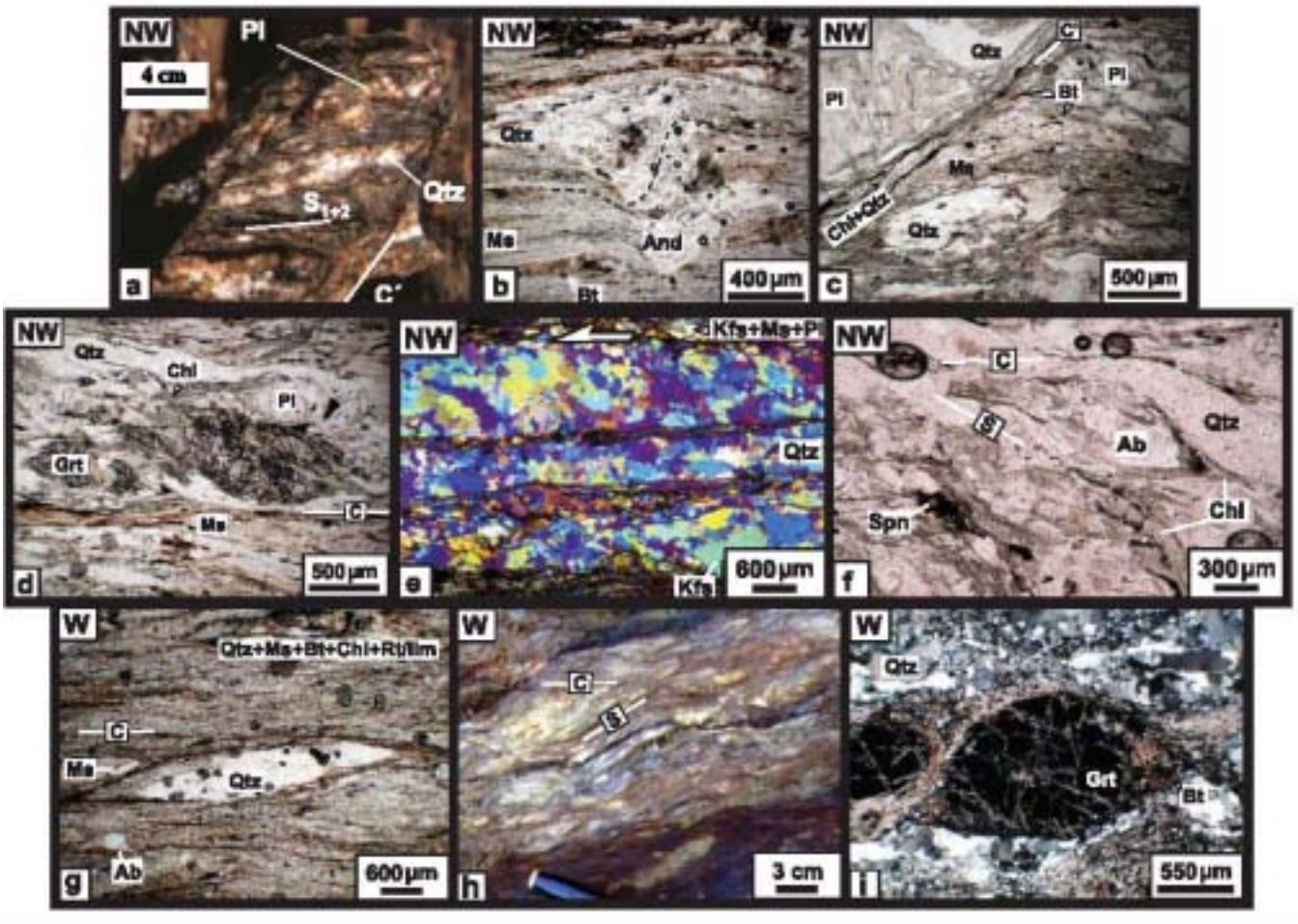

Fig. 7. Microstructures and kinematic criteria from the main shear zones. (a) Lamas de Abad schist, with D_3 C' shear bands cutting S_{1+2} foliation defined by quartz ribbons, plagioclase-rich bands and micaceous domains. (b) Syn-D_3 andalusite porphyroblast from the bottom of the Santiago unit. Rotation path and quartz strain-shadows indicate a top-to-the-NW shearing. (c, d) Phyllonites from the Bembibre detachment shear zone, with an SCC' fabric affecting the gneisses of the Agualada unit (c) and Lamas de Abad schists (d). Relics of previous assemblages are recognized across the fabric, defined by chlorite, quartz and muscovite. (e) Striped gneisses from the top of the Santiago orthogneiss. Dynamically recrystallized quartz ribbons and feldspar muscovite-rich bands define the mylonitic fabric. Oblique foliation defined by preferred orientation of quartz grains shows a top-to-the-NW shearing. SC fabric from the lower slice of the Santiago schists. (f) Albite porphyroblasts with $S_i = S_1$ and σ-shape. Mineral assemblage includes muscovite (Ms), quartz (Qtz), albite (Ab) and titanite (Ttn). (g–i) Mylonites from the Lamas de Abad unit, where SC, mica fish and oblique foliation defined by recrystallized quartz grains point to a top-to-the-east shearing. WM, white mica.

relatively scarce occurrence of biotite in the S_2 orthogneiss fabric may suggest relatively high-P conditions at the beginning of the D_2 event (e.g. Rodríguez Aller 2005). Later, the Santiago orthogneiss was affected by a deformation event, which led to its transformation into an ultramylonitic–phyllonitic fault rock. This change occurred preferentially along the boundaries and includes progressive replacement of D_2 mineralogy by D_3 synkinematic lower-temperature assemblages including chlorite, quartz, epidote, sericite and albite, among other minerals, suggesting greenschist-facies conditions during top-to-the-north shearing (Gómez Barreiro *et al.* 2007).

Kinematic and deformation analyses

The tectonic boundaries of the basal allochthon in the area have been a matter of debate (Van Zuuren 1969; Díaz García 1990; Martínez Catalán *et al.* 2002). The main boundaries have been described as thrusts, low-angle normal faults, extensional detachments and, partially, strike-slip shear zones (Gómez Barreiro *et al.* 2007, and references therein). In a preliminary approach to explain such kinematic variation, the role of the reactivation was explored. It became evident that at least a part of the tectonic contacts in the study area and their regional prolongations along the basal allochthon showed evidence for long-term activity during the Variscan orogeny (Gómez Barreiro *et al.* 2003). Previously defined units appear separated by tectonic boundaries (Figs 4 and 5), most of which developed or were reactivated during D_3.

The kinematic analysis of the tectonic boundaries was carried out in localities where petrological and structural criteria indicate a weak overlapping of the deformation phases. Shear band fabrics (SCC'; Lister & Snoke 1984; Blenkinsop & Treloar 1995) were analysed. The SCC' flow vector ($L_{SCC'}$) (Figs 3 and 5) was calculated plotting the S- and C-plane intersection vectors into a stereoplot, and rotating the intersection vectors 90° within the C or S planes, in SC and SC' fabrics, respectively. This is

Fig. 8. Kinematic criteria in the quarry of Meixonfrío, to the north of Santiago de Compostela, and corresponding to the inner part of the Santiago orthogneiss. The kinematics of D_2 thrust-related ductile shearing is indicated by σ-type porphyroclast systems as being top-to-the-SE (right). The attitude of the mineral lineation is 130°/10° SE. The pen for scale is 8 cm long.

justified because the S planes in SC' fabrics are closer to the general flow plane in the shear zone. Crystallographic preferred orientation of quartz *c*-axes and subgrain boundaries (SGB) were measured in selected quartz-rich tectonites with a universal stage (Fig. 9). Subgrain boundaries lying at a low angle to *c*-axes are consistent with intracrystalline flow parallel to the (0001) quartz basal plane. Stereographic projection of subgrain boundary poles (πSBG) has been considered an approximation to the distribution of quartz *a*-axes (Bouchez 1978; Trépied *et al.* 1980; Okudaira *et al.* 1995). Crystallographic fabrics were processed using Stereo32 v.1.0.1 software (Röller & Trepmann 2008). The macroscopic foliation (S_A) and the shape fabric defined by dynamically recrystallized grains (S_R) were plotted in the stereograms (Knipe & Law 1987). Other criteria were also considered, such as mantled porphyroclasts, mica fish and asymmetric folds, according to the methods developed by Simpson & Schmidt (1983) and Passchier & Trouw (1996). The structural sequence that emerges from the microstructural and kinematic analysis is described below.

First phase (D_1): continental subduction. The subduction-related D_1 kinematics remains somewhat enigmatic, as only indirect evidence such as the regional distribution of metamorphic zones has provided a westward component (in present coordinates) for this episode of continental subduction (Arenas *et al.* 1995; Martínez Catalán *et al.* 1996, 2009). The accompanying metamorphic peak assemblages seem to be preserved in the Santiago unit mainly as an internal foliation ($S_i = S_1$) within albite porphyroblasts. The discontinuous nature of S_i and the strong D_2 overprint prevent the use of this foliation as a D_1 kinematic criterion. This is also the case for the Agualada unit, where only scarce microinclusions in plagioclase may be considered true D_1 fabrics. On the other hand, well-preserved fabrics defined by garnet–white mica–rutile–quartz assemblages in the Lamas de Abad unit point to a high-pressure equilibrium, and represent potential relics of the D_1 kinematics. Structural analysis supports the preservation of a distinct shape fabric (lineation and foliation) across the Lamas de Abad unit (Fig. 5b). Whereas the foliation appears to be oriented almost parallel to the surrounding D_2–D_3 fabrics, the mineral lineation is at high angle to the D_2–D_3 flow directions (Figs 2, 5 and 9), showing a NE–SW trend ($L_1 = 53°/40°$ N; Figs 3 and 5).

SC fabric analysis shows a persistent top-to-the-east sense of shear, with $L_{SC} = 72°/53°$ E on average (Figs 3–5). Quartz *c*-axes show a strong preferred orientation with a pattern defined by a single peripheral maximum close to the pole of the shear zone boundary and the mylonitic foliation (e.g. GB 3, Fig. 9). The top-to-the-east monoclinic symmetry is also supported by the preferred orientation of subgrain boundaries, which geometrically correlate with the *a*-axes. Quartz *c*-axis patterns suggest that a simple shear component dominated during the fabric development. This is in accordance with the scarce development of C'C" shear bands. Quartz crystallographic fabrics may be interpreted in terms of dominant intracrystalline slip systems, so we could make some suggestions about deformation conditions (e.g. Lister *et al.* 1978; Law *et al.* 1994). Classical interpretation of *c*- and *a*-axis patterns suggests that slip on basal <*a*> slip and minor rhomb <*a*> systems may be active during deformation (e.g. Schmid & Casey 1986). Thermal conditions of this intracrystalline flow are consistent with the metamorphic evolution described previously (e.g. Okudaira *et al.* 1995; Kurz *et al.* 2002; Toy *et al.* 2008).

Mica fish, mantled σ- and δ-type porphyroclasts and asymmetric microfolds also support the same kinematics (Fig. 7g and i). It should be noted that garnet porphyroblasts show a snowball geometry with S_i defined, for example, by rutile in continuity with the external foliation, where rutile is also stable. Garnet shows δ and σ shapes, which may suggest some ductile behaviour of this mineral. All these features suggest that the mylonitic fabric in the Lamas de Abad sector was developed under high-*P* conditions. However, we are aware that partial re-equilibration of the fabric towards lower-pressure conditions during the beginning of the exhumation process may mask D_1 kinematics. Additionally, initial D_2 stages in the area might have also developed under general high-*P* (>12 kbar) conditions, as documented for structurally equivalent domains in other segments across the upper sequence in the basal allochthon (Arenas *et al.* 1995; López Carmona *et al.* 2010). In that sense, the Lamas de Abad fabrics should be considered transient between D_1 and D_2 (S_{1+2}; Fig. 6c). This is also consistent with variations in flow direction between top-to-the-NE and top-to-the-SE shearing (Fig. 5).

Second phase (D_2): thrust-related exhumation. This stage led to the development of a regional fabric along the basal allochthon in the upper and lower sequences. In the Agualada unit, the main fabric was established during this stage under general amphibolite-facies conditions. This is also recognized at some levels of the Lamas de Abad unit, where the main foliation partially re-equilibrated the D_1 assemblages with a conspicuous biotite growth from garnet. In the Santiago unit, a pervasive schistosity (S_2) was generated in the schists, defined by muscovite, biotite, syntectonic albite porphyroblasts and chlorite (Fig. 6h and i). A slightly higher grade is recognized in schists above the Santiago orthogneiss. Ribbons of dynamically recrystallized quartz are locally abundant (Fig. 7e).

The main fabric in the Santiago orthogneiss developed at that time. Central regions of the orthogneiss exhibit coarse-grained types, where a foliation roughly parallel to its boundaries is defined by white mica, augen feldspars and garnet. Surrounding these areas, mylonitic gneisses with quartz and feldspar ribbons developed (Fig. 7e). Consistent kinematic criteria exist within the inner sectors of the Santiago orthogneiss where SC and σ-type

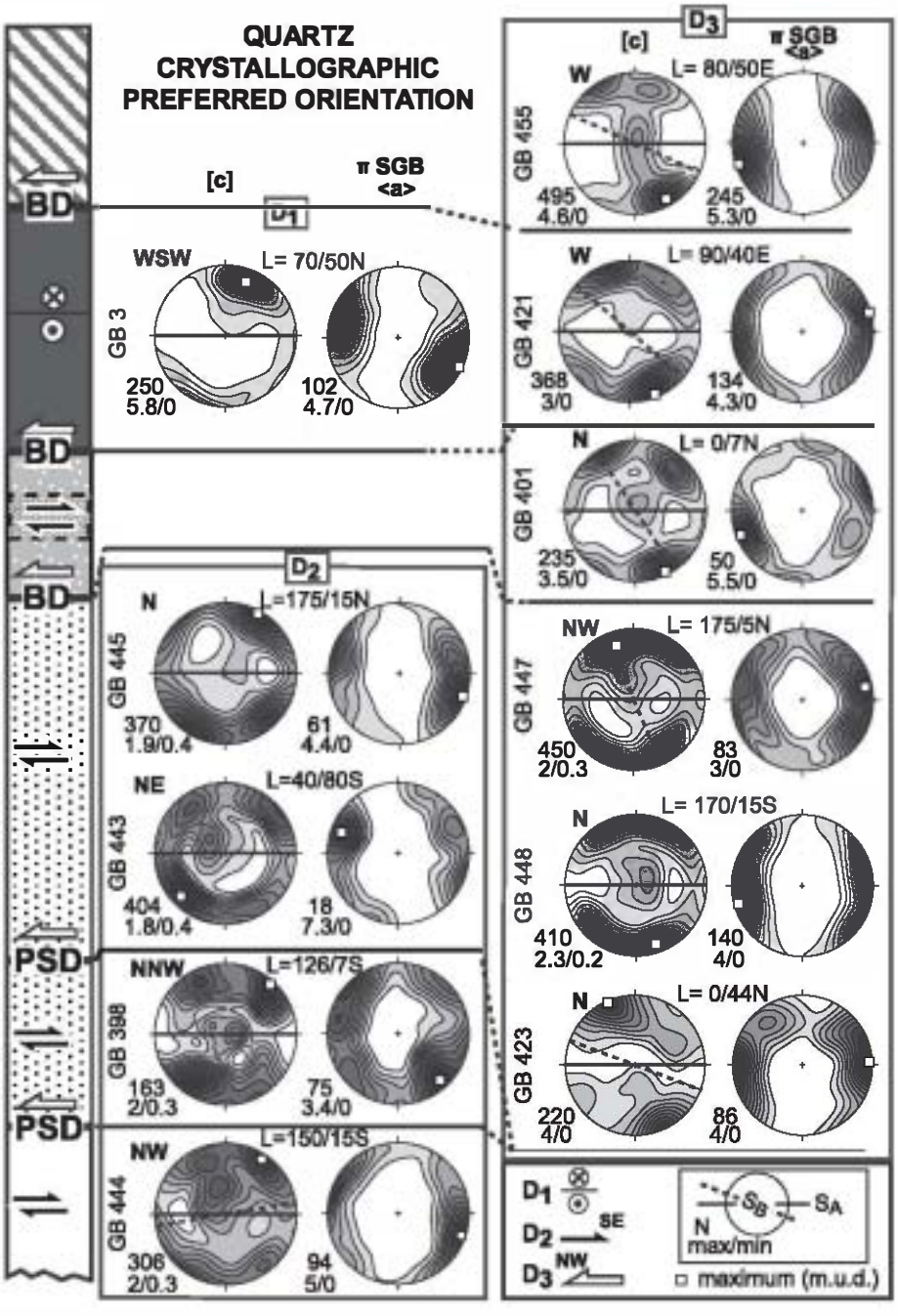

Fig. 9. Selected quartz *c*-axes and subgrain boundary (πSGB ~ <*a*>) pole figures, measured on the universal stage. Results are shown in a synthesis column where the main tectonic boundaries are included. Code for units as in Figure 3. Equal area, lower hemisphere projections. Density distribution scaled to multiples of the uniform distribution (m.u.d.). □, maximum density. Main foliation (S_A) and oblique foliation (S_B) defined by recrystallized quartz are also indicated. Pole figures are grouped into deformation phases D_1, D_2 and D_3.

porphyroclast systems show a general top-to-the-south or -SE sense of shear (Fig. 8). The trend of D_2 mineral lineation varies between NW SE and north south (Figs 2 5). To the south, shear zones crop out below the Pico Sacro detachment displaying a clear top-to-the-SE kinematics, as defined by SCC' fabrics (L_{SCC} = 135°/20° SE).

Evidence of D_2 flow has been found also in quartz fabrics across the unit, mainly in the lower part of the Santiago schists (D_2; Fig. 9). D_2 fabrics share complex quartz *c*-axis patterns where partially connected girdles and submaxima define a quasi-orthorhombic symmetry, suggesting flattening perpendicular to the foliation plane. However, density distribution and the orientation of subgrain boundary poles point to a rotational component of the flow, with a monoclinic symmetry, reflecting a top-to-the-SSE shearing. This is also confirmed by oblique foliation in quartz ribbons, and mica fish. Most of the subgrain boundary poles and *c*-axes are orthogonal (Fig. 9), so we could consider them a qualitative approximation to *a*-axes. Altogether, quartz *c*-axis fabric and SC'C" shear band development point to a stretching shearing behaviour (Passchier & Trouw 1996). At a regional scale, this phase has been related to top-to-the-SE exhumation of the basal allochthon driven by major recumbent folding and thrusting (Martínez Catalán *et al.* 1996; Díez Fernández & Martínez Catalán 2009).

Third phase (D_3): exhumation during extensional collapse. During this phase most of the rocks in the basal allochthon were affected by ductile deformation, which resulted in retrogression

of the D_2 assemblages. This deformation is closely related to two distinct extensional structures, the Bembibre and Pico Sacro detachments.

The Bembibre detachment. This is a broad, heterogeneous shear zone characterized by the development of a phyllonitic network, which is especially pervasive at the top of the sequence, where it affects the Agulada and Lamas de Abad units (Figs 2 5). Similar features appear heterogeneously distributed across the Santiago schists downward. Mylonitic S_3 fabrics anastomose around less deformed domains of the Agualada and Lamas de Abad units (Fig. 5). In the Santiago orthogneiss, mylonitic bands and phyllonites form close to the boundary with the schists (Fig. 5). Whereas schistose lithologies display a penetrative SCC' fabric, the orthogneiss evolved from striped gneisses to phyllonites.

The mineral lineation across the phyllonitic network and mylonites shows a persistent NNW SSE trend, although variations may occur as a result of interference of shear zones, rigid rotation of blocks between them, and late folding (Figs 2 and 3). D_3 deformation progressively concentrated from the initial 1 km width high-strain zone to discrete metre-size shear zones along boundaries where mechanical contrasts exist, such as the uppermost contact with the upper allochthon, and the schist orthogneiss boundary (Figs 4 and 5). Ductile flow in the Bembibre detachment affects not only the basal allochthon but also the upper allochthon (Gómez Barreiro 2007), where overturned drag folds with west vergence developed in the vicinity of the detachment (Figs 2 4 and 10). Along the upper boundary, metre-scale lenses of talc-schists occur, suggesting that ultramafic lithologies, probably corresponding to the ophiolitic allochthon, were also affected and removed by this structure (Gómez Barreiro 2007).

The analysis of D_3 shear bands indicates a persistent top-to-the-NW sense of shear, with NNW SSE L_{SC} vectors on average (Fig. 3). Other microstructures, such as mica fish and σ-type porphyroclast systems, support this kinematics (Fig. 7a, c and d). It is relatively common to find in both schists and orthogneisses an oblique foliation defined by dynamically recrystallized quartz grains (S_B) along the ribbons. This microstructure indicates a dominant top-to-the-NW sense of shear.

Quartz *c*-axis fabrics have complex patterns that range from single maxima to partially connected crossed girdles (D_3; Fig. 9). Most of the samples tend to develop symmetrical patterns with respect to the reference frame. Deviations from that tendency include external and internal asymmetries resulting in consistent top-to-the-NW shearing. The analysis of the subgrain boundaries in quartz supports the existence of this rotational component in the deformation flow (Fig. 9). The sense of shear is consistent with top-to-the-NNW criteria. The association of microstructures and quartz fabrics is compatible with a combination of simple and pure shear during the activity of the Bembibre detachment, which may be considered a stretching shear zone. The existence of a stretch component parallel to the direction of the flow correlates also with the dramatic thinning of the Santiago orthogneiss to the south.

Geometric analysis of drag folds formed in the hanging wall to the Bembibre detachment can be used to derive kinematic information (Ramsay & Huber 1987; Wheeler 1987; Passchier & Williams 1996). Minor and major flexures were systematically examined along the contact (Figs 3 and 4). The results include north south to west east fold axes, with a general vergence to the NW. If we consider the projection of the normal to the fold axes on the fault plane as a slip vector, a consistent top-to-the-NW movement (121°/24° SE) can be established (Fig. 3). Towards the bottom of the Santiago unit, the abundance of phyllonites and of kinematic criteria related to the Bembibre detachment decreases, partially deleted by the motion of the Pico Sacro detachment.

The Pico Sacro detachment. This extensional structure partially overprints the Bembibre detachment (Fig. 4). Along the Pico Sacro detachment low-grade brittle ductile to brittle deformation dominates. However, relicts of an early ductile behaviour under higher-grade conditions can be noticed. They consist of low-pressure, high- to intermediate-temperature assemblages at

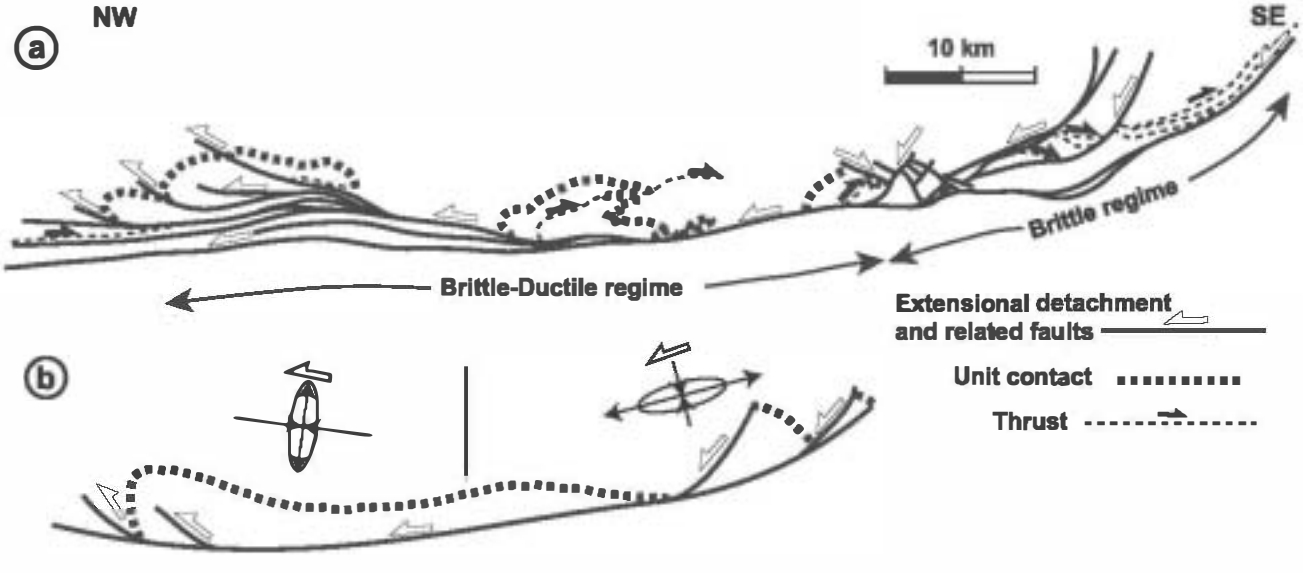

Fig. 10. (a) The Bembibre and Pico Sacro detachments unfolded, showing their mutual relationships and associated structures. Deformation mechanisms indicate that the Pico Sacro detachment cuts progressively higher structural levels to the SE, where normal listric and conjugate faults occur. To the NW, in the direction of movement of the hanging wall, drag folds and reverse faults developed above the Bembibre detachment. (b) Mega-slump model explaining extension at the upper structural levels and shortening at depth in the Bembibre–Pico Sacro detachment system. Based on Gómez Barreiro *et al.* (2002).

the bottom of the Santiago unit (Van Zuuren 1969; Gómez Barreiro 2007), where andalusite porphyroblasts with sigmoidal inclusions indicate about 45° of sinistral rotation with respect to the external schistosity (Fig. 7b). Asymmetric strain shadows are also present, suggesting a top-to-the-NW shearing, and indicating a syn-D_3 character for this thermal event.

Later evolution of the Pico Sacro detachment has been explored focusing on major cross-cutting relationships with the Bembibre detachment and distinct fault planes where only the Pico Sacro detachment-related structures are recognized. The shear zone widths range from some decimetres to metres. Phyllonites represent the ductile expression of the detachment at that stage. It is common to find that frictional fault rocks and ductile fault rocks overlap along the fault plane. Moreover, a quartz vein or dyke several kilometres long appears along the Pico Sacro detachment (Fig. 2). As was pointed out by Gómez Barreiro (2007), the Pico Sacro detachment fault plane acted as a pathway for fluids (Sibson 1990; Bons 2001). Massive input of fluids along the fault may explain the origin of the Pico Sacro quartz vein. Following the Pico Sacro detachment to the east only frictional fault rocks define the fault plane, whereas conjugate and listric normal faults cut across the hanging-wall units, ending at the Pico Sacro detachment fault plane (Figs 1, 2 and 10). These features may suggest that shallower structural levels crop out to the east (Gómez Barreiro 2007).

Low- to very low-grade conditions dominated the late activity of the Pico Sacro detachment. Discrete phyllonitic zones associated with the Bembibre detachment could have nucleated the Pico Sacro detachment, evolving later to a more fragile structure. C' shear bands show a top-to-the-NW sense of shear. Shear sense indicators in cataclasites, including Riedel shears, quartz veins and scarce shear bands in foliated cataclasites, are consistent with that sense of shear (Chester *et al.* 1985; Evans 1990; Passchier & Trouw 1996).

Quartz *c*-axis fabrics measured within the Pico Sacro detachment show an almost symmetrical pattern, close to a type I cross girdle (Fig. 9; Lister 1977; Schmid & Casey 1986). However, density distribution and preferred orientation of subgrain boundaries define a monoclinic pattern. These features are consistent with top-to-the-north shearing and may have developed through a combination of pure and simple shear.

A displacement of roughly 20 km can be estimated for the Bembibre and Pico Sacro detachments if the Santiago orthogneiss is correlated with comparable felsic orthogneisses eastward, in lower sequence units such as the Lalín unit (Fig. 1). Both extensional structures were later affected by north south open, subvertical folds, and partially cut by transcurrent shear zones (Figs 1 and 2). In the study area, a sinistral steeply dipping shear zone defines a high-strain band that deforms Variscan granites and the lower contact of the basal allochthon. In the footwall to the Pico Sacro detachment, sinistral SC bands developed in granitoids, displaying L_{SC} vectors around 150°/10° N. Similar structures have been described for all of the allochthonous complexes in the NW Iberian Massif (Iglesias Ponce de León & Choukroune 1980).

Age of tectonometamorphic events

The basal allochthon followed a complex tectonic evolution from early burial stages in a subduction zone until the readjustments leading to crustal equilibration. According to available geochronological data, 370 Ma may be considered an upper bound for the subductive event (D_1), which probably ended around 365 Ma (Rodríguez *et al.* 2003; Abati *et al.* 2010). The exhumation under amphibolite-facies conditions driven by thrusting and recumbent folding directed to the SE (D_2) is constrained by the Lalín Forcarei thrust activity. This is considered to be the main thrust responsible for the emplacement of the basal allochthon, being active around 340 Ma (Martínez Catalán *et al.* 1996; Dallmeyer *et al.* 1997) and later in any case than migmatization in the Agualada unit, dated at 346 Ma (Abati & Dunning 2002). This stage overlapped that of recumbent folding and resulted in a thickening of the orogenic crust at a regional scale.

The Bembibre Pico Sacro detachment system was active during widespread partial melting and the emplacement of synkinematic granitoids (Gómez Barreiro *et al.* 2003, 2007; Martínez Catalán *et al.* 2009). Its activity may be constrained between 340 Ma and 323 ± 11 or 317 ± 15 Ma, the age of cross-cutting Variscan granitoids (Bellido *et al.* 1992; Ortega Cuesta 1998). Unfortunately, no direct dating of D_3 deformation fabrics exists to date, but we could find structural counterparts of the Bembibre Pico Sacro detachment system at middle- to lower-crustal levels, where partial melting, related to the gravitational collapse of the orogen, appears to have occurred in gneiss domes around 320–310 Ma (Díez Montes 2007). A direction roughly parallel to the orogenic trend has been found to be a relevant flow direction in those structures (Escuder Viruete *et al.* 1994; Díez Balda *et al.* 1995; Díez Montes 2007).

Summary and discussion

A new tectonometamorphic sequence has been identified in the basal allochthon. A high-grade lens in the uppermost part, with migmatitic paragneisses and granitic orthogneisses, may be correlated with the Agualada unit to the north, on the basis of metamorphic conditions and lithological association (Arenas *et al.* 1997). The Lamas de Abad unit below shows a clear linkage with the upper sequences of the basal allochthon to the west (Malpica–Tui unit), the so-called Ceán unit (Díez Fernández *et al.* 2010; López Carmona *et al.* 2010). The best-preserved mineral assemblages in the area suggest equilibrium under high-P conditions (D_1), with a later re-equilibration under intermediate-P and lower-T conditions (D_2; greenschist facies) (López Carmona *et al.* 2010). Structural and kinematic analysis of these rocks suggests that a strong shearing occurred prior to the re-equilibration with a general top-to-the-ENE sense of motion.

The Santiago unit occupies the lowermost structural position of the basal units. High-pressure relics (D_1) appearing as microinclusions within syn-D_2 albite porphyroblasts are witnesses of an early episode of subduction. Subsequently, the development of S_2 could be related to a general top-to-the-SE shearing. D_2 mineral assemblages suggest that an inverted thermal gradient did occur in the area, as described by Arenas *et al.* (1995) in the north. These data are clearly correlated with the first exhumation event identified in other sectors of the basal allochthon, which was accomplished via recumbent folding and thrusting (Arenas *et al.* 1995; Martínez Catalán *et al.* 1996; Díez Fernández & Martínez Catalán 2009).

A later deformation stage (D_3) resulted in a kinematic change with a persistent top-to-the-NW sense of shear, with the formation of the major Bembibre and Pico Sacro detachments. Previous mineral assemblages appear heterogeneously retrogressed, with the development of anastomosed phyllonitic bands across the unit. Field relationships (Figs 2, 4 and 5) show that the Santiago schists on top of the Santiago orthogneiss, Lamas de Abad and Agualada units are lens-shaped and bounded by low-dipping normal faults. This and the absence of the ophiolitic

allochthon support the subtractive character of the detachment system.

Deformation conditions may be inferred from mineral variations and microstructural evolution. Previous high-*P* mineral assemblages turned into amphibolite- and greenschist-facies parageneses. Downward in the basal allochthon, a low-*P* heating event developed, and has been kinematically linked to D_3. It seems to be related to the formation of migmatitic domes, which are common at deep levels in the autochthon and Schistose Domain, and associated with the extensional collapse of the orogenic belt (Martínez Catalán *et al.* 2009). Microstructures and fabric symmetry provided by structural analysis of the detachment system indicate that a general shear (Hanmer & Passchier 1991), that is, a combination of simple and pure shear components, with stretching parallel to the flow direction, is appropriate to describe the ductile deformation flow during the activity of the detachments.

For the brittle counterpart, deformation mechanisms in the Pico Sacro detachment indicate progressively higher structural levels to the SE. This implies an original dip towards the NE, coincident with the hanging-wall motion (Fig. 10a), which reinforces the interpretation of the Pico Sacro detachment as a huge normal fault. Normal listric and conjugate faults occur to the SE of the Pico Sacro detachment, whereas drag folds and reverse faults developed above the Bembibre detachment to the NW. The distributions of these associated structures are similar to those found on mega-slumps (Webb & Cooper 1988), which, like the Bembibre Pico Sacro detachment system, may have undergone extension in the upper structural levels and shortening at depth (Fig. 10b).

Taking into account isotopic ages and overlapping relationships, we suggest a conceptual model (Fig. 11) in which crustal thickening during D_2 was followed by thermal relaxation. This resulted in temperature increase and partial melting during D_3, which facilitated the ductile flow that accomplished gravitational extension in the lower to middle crust (Vanderhaege & Teyssier 2001; Gómez Barreiro *et al.* 2007; Martínez Catalán *et al.* 2009). The mechanisms responsible for transferring this flow to the upper crust are often obscure, but in our case, the Bembibre Pico Sacro system seems to be the upper crustal expression of the late orogenic extensional collapse. The detachments would act as a rheological boundary between the upper part of the orogenic pile, here represented by the ophiolitic and upper allochthons, which behaved rigidly, and the ductile middle crust (Fig. 11).

In spite of cross-cutting relationships between the Bembibre and Pico Sacro detachments (Fig. 10a), they seem to represent a continuous process, which evolved from medium- to low-grade and, finally, to very low-grade conditions. Extensional shear zones preferentially concentrate in the upper part of the structural sequence of the basal allochthon, where a previous, top-to-the-ENE thrust-related high-strain shear zone existed. Its presence may have favoured the nucleation of the Bembibre detachment, which would have reactivated older fabrics. Moreover, the deformation regime in the D_3 detachment system also evolved, as documented by the overprinting of dominant ductile (Bembibre detachment) to brittle ductile or brittle fault rocks (Pico Sacro detachment).

The basal allochthon concentrated important displacements of the allochthonous complexes during the Variscan orogeny. Although renewal of pre-existing features, such as lithological contacts and/or shear zones, is derived from our data, precise dating of each deformation stage would provide the clues to differentiate true reactivation from a continuous event (Butler *et al.* 1997; Miller *et al.* 2001). In any case, our data support a strong influence of the pre-existing tectonothermal architecture on the deformational response of the basal allochthon. It is proposed that the basal allochthon may be considered a crustal volume where tectonic reworking was concentrated for at least 50 Ma.

Conclusions

The structural and kinematic analysis carried out in the basal allochthon of the southwestern part of the Órdenes Complex has resulted in the identification of the Santiago, Lamas de Abad and

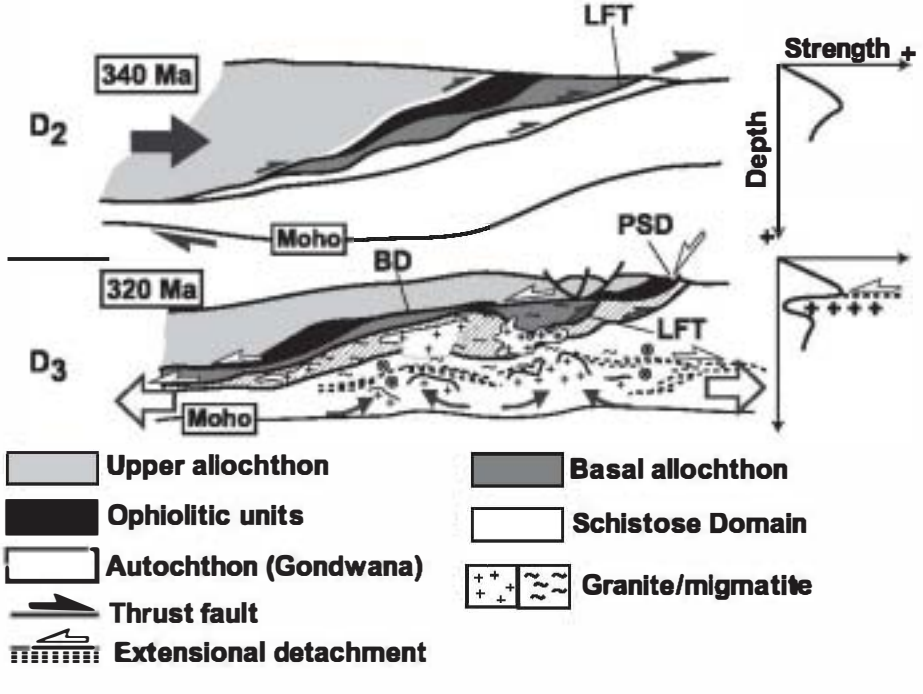

Fig. 11. Conceptual model (not to scale) of the exhumation of the basal allochthon in the area. D_2 stage results in the exhumation of the basal units through a combination of thrusting and recumbent folding. Early stages may have developed under high-*P* conditions. The Lalín–Forcarei thrust (LFT) represents the most significant thrust fault with an eastward kinematics. Later, D_2 shortening associated with the underthrusting of Gondwana basement developed an out-of-sequence thrust system that barely dismembered the basal allochthon (Gómez Barreiro *et al.* 2007; Martínez Catalán *et al.* 2009). After D_2 thickening, thermal relaxation led to widespread melting of the lower and middle crust, during D_3. The orogenic pile became mechanically unstable, resulting in an extensional collapse. Whereas domes and viscous flow developed at depth, extensional detachments nucleated at the base of the rigid upper crustal segments. The Bembibre and Pico Sacro detachments (BD, PSD) are representative of this evolution.

Agualada units, of which the last two have not been described before. The tectonometamorphic evolution that we found led us to assign these units to two distinct parts of the basal allochthon: the upper sequence (Lamas de Abad unit) and the lower sequence (Santiago and Agualada units). An episode of thrusting related to a collisional stage led to the development of an inverted metamorphic gradient, and the duplication of lower sequence units. A similar relationship could be extended to the north in the Órdenes Complex.

Three main tectonic phases are responsible for the configuration of the basal allochthon. The first was a high-pressure event related to the subduction of the whole ensemble, D_1, the late stages of which seem to be preserved in the Lamas de Abad unit, where a top-to-the-ENE sense of shear has been recognized. This kinematics is consistent with a subduction component to the west in present coordinates previously inferred from the distribution of high-*P* metamorphic zoning. A second, amphibolite-facies event with top-to-the-SE kinematics and related to the regional exhumation of the units through thrusting and recumbent folding, D_2, is widely distributed in the three units. The third phase, D_3, occurred under retrogressive amphibolite- to greenschist-facies conditions, and resulted in the development of the Bembibre Pico Sacro detachment system, a regional-scale extensional framework with deformation distributed heterogeneously and top-to-the-NW kinematics.

The structural position and fault-rock evolution suggest that the Bembibre Pico Sacro system partially rejuvenated pre-existing shear zones, whose weakness may have favoured the nucleation of the detachments by reactivation of older fabrics. During this phase, syntectonic low-*P* and high- to medium-*T* assemblages formed at the bottom of the basal allochthon. Later in D_3, the Pico Sacro detachment cut across the Bembibre detachment under greenschist-facies conditions and a viscous to frictional regime. According to the cross-cutting relationships and regional geology, the Bembibre Pico Sacro system is coeval with late orogenic extensional collapse and widespread magmatism, and represents its upper-crustal expression. The detachments correlate with mid- and lower-crustal flow and the development of gneiss domes at depth.

Therefore, the basal allochthon analysed here can be considered as an orogenically reworked crustal ensemble representing a rheological boundary layer between the more rigid upper allochthon above and the more viscous Schistose Domain and autochthon below.

This work is dedicated to the memory of F. Díaz García, a remarkable scientist and an outstanding person. His mentorship, friendship and support will be greatly missed. Funding was provided by the Dirección General de Programas y Transferencia del Conocimiento (Spanish Ministry of Science and Innovation), research project CGL2007-65338-C02-01 and -02/BTE. J.G.B. was supported by MEC-Juan de la Cierva Postdoctoral contract. We are grateful to S. Smith, J. von Raumer and an anonymous referee for thorough and constructive reviews, and to K. McCaffrey for the editorial work.

References

Abati, J. & Dunning, G.R. 2002. Edad U–Pb en monacitas y rutilos de los paragneises de la Unidad de Agualada (Complejo de Órdenes, NW del Macizo Ibérico). *Geogaceta*, **32**, 95–98.

Abati, J., Arenas, R., Martínez Catalán, J.R. & Díaz García, F. 2003. Anticlockwise *P–T* path of granulites from the Monte Castelo Gabbro (Órdenes Complex, NW Spain). *Journal of Petrology*, **44**, 305–327.

Abati, J., Gerdes, A., Fernández-Suárez, J., Arenas, R., Whitehouse, M.J. & Díez Fernández, R. 2010. Magmatism and early-Variscan continental subduction in the northern Gondwana margin recorded in zircons from the basal units of Galicia, NW Spain. *Geological Society of America Bulletin*, **122**, 219–235.

Andonaegui, P., González del Tánago, J., Arenas, R., Abati, J., Martínez Catalán, J.R., Peinado, M. & Díaz García, F. 2002. Tectonic setting of the Monte Castelo gabbro (Ordenes Complex, northwestern Iberian Massif): Evidence for an arc-related terrane in the hanging wall to the Variscan suture. *In:* Martínez Catalán, J.R., Hatcher, R.D., Jr, Arenas, R. & Díaz García, F. (eds) *Variscan–Appalachian Dynamics: the Building of the Late Paleozoic Basement*. Geological Society of America, Special Papers, **364**, 37–56.

Arenas, R., Rubio Pascual, F.J., Díaz García, F. & Martínez Catalán, J.R. 1995. High-pressure micro-inclusions and development of an inverted metamorphic gradient in the Santiago Schists (Ordenes Complex, NW Iberian Massif, Spain): evidence of subduction and syn-collisional decompression. *Journal of Metamorphic Geology*, **13**, 141–164.

Arenas, R., Abati, J., Martínez Catalán, J.R., Díaz García, F. & Rubio Pascual, F.J. 1997. *P–T* evolution of eclogites from the Agualada Unit (Ordenes Complex, NW Iberian Massif, Spain): Implications for crustal subduction. *Lithos*, **40**, 221–242.

Arenas, R., Martínez Catalán, J.R., Sánchez Martínez, S., *et al.* 2007. Paleozoic ophiolites in the Variscan suture of Galicia (northwest Spain): distribution, characteristics and meaning. *In:* Hatcher, R.D., Jr, Carlson, M.P., McBride, J.H. & Martínez Catalán, J.R. (eds) *4-D Framework of Continental Crust*. Geological Society of America, Memoirs, **200**, 425–444, doi:10.1130/2007.1200(22).

Bellido, F., Brandle, J.L., Lasala, M. & Reyes, J. 1992. Consideraciones petrológicas y cronológicas sobre las rocas graníticas hercínicas de Galicia. *Cuadernos do Laboratorio Xeolóxico de Laxe*, **17**, 241–261.

Berthé, D., Choukroune, P. & Jegouzo, P. 1979. Orthogneisses, mylonite and non coaxial deformation of granites: the example of the South Armorican Shear Zone. *Journal of Structural Geology*, **1**, 31–42.

Blenkinsop, T.G. & Treloar, P.J. 1995. Geometry, classification and kinematics of S–C and S–C' fabrics in the Mushandike area, Zimbabwe. *Journal of Structural Geology*, **17**, 397–408.

Bons, P. 2001. The formation of large quartz veins by rapid ascent of fluids in mobile hydrofiactures. *Tectonophysics*, **336**, 1–17.

Bouchez, J.L. 1978. Preferred orientation of quartz <*a*> axes in some tectonites: kinematic inferences. *Tectonophysics*, **49**, 25–30.

Butler, R.W.H., Holdsworth, R.E. & Lloyd, G.E. 1997. The role of basement reactivation in continental deformation. *Journal of the Geological Society, London*, **154**, 69–71.

Castiñeiras, P. 2005. *Origen y evolución tectonoternal de las unidades de O Pino y Cariño (Complejos Alóctonos de Galicia)*. Laboratorio Xeolóxico de Laxe, Serie Nova Terra, **28**.

Castiñeiras, P., Díaz García, F. & Gómez Barreiro, J. 2010. REE-assisted U–Pb zircon age (SHRIMP) of an anatectic granodiorite: Constraints on the evolution of the A Silva granodiorite, Iberian Allochthonous Complexes. *Lithos*, doi:10.1016/j.lithos.2010.01.013.

Chester, F.M., Friedman, M. & Logan, J.M. 1985. Foliated cataclasites. *Tectonophysics*, 111, 134–146.

Dallmeyer, R.D., Martínez Catalán, J.R., Arenas, R., *et al.* 1997. Diachronous Variscan tectonothermal activity in the NW Iberian Massif: Evidence from $^{40}Ar/^{39}Ar$ dating of regional fabrics. *Tectonophysics*, **277**, 307–337.

Díaz García, F. 1990. *La geología del sector occidental del Complejo de Ordenes (Cordillera Hercínica, NW de España)*. Laboratorio Xeolóxico de Laxe, Serie Nova Terra, **3**.

Díaz García, F., Arenas, R., Martínez Catalán, J.R., González del Tánago, J. & Dunning, G. 1999. Tectonic evolution of the Careón ophiolite (Northwest Spain): a remnant of oceanic lithosphere in the Variscan belt. *Journal of Geology*, **107**, 587–605.

Díez Balda, M.A., Martínez Catalán, J.R. & Ayarza, P. 1995. Syn-collisional extensional collapse parallel to the orogenic trend in a domain of steep tectonics: the Salamanca detachment zone (Central Iberian Zone, Spain). *Journal of Structural Geology*, **17**, 163–182.

Díez Fernández, R. & Martínez Catalán, J.R. 2009. 3D analysis of an Ordovician igneous ensemble: A complex magmatic structure hidden in a polydeformed allochthonous Variscan Unit. *Journal of Structural Geology*, **31**, 222–236.

Díez Fernández, R., Martínez Catalán, J.R., Verdes, A., Abati, J., Arenas, R. & Fernández-Suárez, J. 2010. U–Pb ages of detrital zircons from the Basal allochthonous units of NW Iberia: Provenance and paleoposition on the northern margin of Gondwana during the Neoproterozoic and Paleozoic. *Gondwana Research*, doi:10.1016/j.gr.2009.12.006.

Díez Montes, A. 2007. *La Geología del Dominio 'Ollo de Sapo' en las comarcas de Sanabria y Terra do Bolo*. Laboratorio Xeolóxico de Laxe, Serie Nova Terra, **34**.

Escuder Viruete, J., Arenas, R. & Martínez Catalán, J.R. 1994. Tectonother-

mal evolution associated with Variscan crustal extension in the Tormes Gneiss Dome (NW Salamanca, Iberian Massif, Spain). *Tectonophysics*, **238**, 117–138.

Evans, J.P. 1990. Textures, deformation mechanisms and the role of fluids in the cataclastic deformation of granite rocks. *In:* Knipe, R.J. & Rutter, E.H. (eds) *Deformation Mechanisms, Rheology and Tectonics*. Geological Society, London, Special Publications, **54**, 29–39.

Farias, P., Gallastegui, G., González-Lodeiro, F., *et al.* 1987. Aportaciones al conocimiento de la litoestratigrafía y estructura de Galicia Central. *Memórias da Faculdade de Ciências, Universidade do Porto*, 1, 411–431.

Gil Ibarguchi, I. & Ortega Gironés, E. 1985. Petrology, structure and geotectonic implications of glaucophane-bearing eclogites and related rocks from the Malpica–Tuy (MT) Unit, Galicia, Northwest Spain. *Chemical Geology*, **50**, 145–162.

Gómez Barreiro, J. 2007. *La Unidad de Fornás: Evolución tectonometamórfica del SO del Complejo de Órdenes*. Laboratorio Xeolóxico de Laxe, Serie Nova Terra, **32**.

Gómez Barreiro, J., Martínez Catalán, J.R., Arenas, R. & Díaz García, F. 2002. Caracterización cinemática del contacto inferior de la Unidad de Fornás (Complejo de Órdenes, NW del Macizo Ibérico). *Studia Geologica Salmanticensia*, **38**, 105–127.

Gómez Barreiro, J., Martínez Catalán, J.R. & Arenas, R. 2003. Reactivation of a major tectonic boundary: preservation of crystallographic fabrics. *In: Deformation Mechanisms, Rheology and Tectonics. St. Malo (France), Abstracts*, 65.

Gómez Barreiro, J., Wijbrans, J.R., Castiñeiras, P., Martínez Catalán, J.R., Arenas, R., Díaz García, F. & Abati, J. 2006. $^{40}Ar/^{39}Ar$ laserprobe dating of mylonitic fabrics in a polyorogenic terrane of the NW Iberia. *Journal of the Geological Society, London*, **163**, 61–73.

Gómez Barreiro, J., Martínez Catalán, J.R., Arenas, R., Castiñeiras, P., Abati, J., Díaz García, F. & Wijbrans, J.R. 2007. Tectonic evolution of the upper allochthon of the Órdenes Complex (northwestern Iberian Massif): structural constraints to a polyorogenic peri-Gondwanan terrane. *In:* Linnemann, U., Nance, R.D., Kraft, P. & Zulauf, G. (eds) *The Evolution of the Rheic Ocean: from Avalonian–Cadomian Active Margin to Alleghenian–Variscan Collision*. Geological Society of America, Special Papers, **423**, 315–332.

Gómez Barreiro, J., Martínez Catalán, J.R., Prior, D., *et al.* 2010. Fabric development in a middle Devonian intraoceanic subduction regime: the Careón ophiolite (northwest Spain). *Journal of Geology*, **118**, 163–186.

Hanmer, S. & Passchier, C.W. 1991. *Shear Sense Indicators: a Review*. Geological Survey of Canada Papers, **90**.

Holdsworth, R.E., Butler, C.A. & Roberts, A.M. 1997. The recognition of reactivation during continental deformation. *Journal of the Geological Society, London*, **154**, 73–78.

Holdsworth, R.E., Hand, M., Miller, J.A. & Buick, I.S. 2001. Continental reactivation and reworking: an introduction. *In:* Miller, J.A., Holdsworth, R.E., Buick, I.S. & Hand, M. (eds) *Continental Reactivation and Reworking*. Geological Society, London, Special Publications, **184**, 1–12.

Houseman, G.A. & Molnar, P. 2001. Mechanisms of lithospheric renewal associated with continental orogeny. *In:* Miller, J.A., Holdsworth, R.E., Buick, I.S. & Hand, M. (eds) *Continental Reactivation and Reworking*. Geological Society, London, Special Publications, **184**, 13–37.

Iglesias Ponce de León, M. & Choukroune, P. 1980. Shear zones in the Iberian arc. *Journal of Structural Geology*, **2**, 63–68.

Knipe, R.J. & Law, R.D. 1987. The influence of crystallographic orientation and grain boundary migration on microstructural and textural development in a S–C mylonite. *Tectonophysics*, **135**, 155–169.

Kurz, W., Fritz, H., Tenczer, V. & Unzog, W. 2002. Tectonometamorphic evolution of the Koralm Complex (Eastern Alps): constraints from microstructures and textures of the 'Plattengneis' shear zone. *Journal of Structural Geology*, **24**, 1957–1970.

Law, R.D., Miller, E.L., Little, T.A. & Lee, J. 1994. Extensional origin of ductile fabrics in the Schist Belt, Central Brooks Range, Alaska—II. Microstructural and petrofabric evidence. *Journal of Structural Geology*, **16**, 919–940.

Lister, G.S. 1977. Discussion: crossed-girdle *c*-axis fabrics in quartzites plastically deformed by plane strain and progressive simple shear. *Tectonophysics*, **39**, 51–54.

Lister, G.S. & Snoke, A.W. 1984. S–C mylonites. *Journal of Structural Geology*, **6**, 617–638.

Lister, G.S., Paterson, M.S. & Hobbs, B.E. 1978. The simulation of fabric development in plastic deformation and its application to quartzite: the model. *Tectonophysics*, **45**, 107–158.

López Carmona, A., Abati, J. & Reche, J. 2010. Petrologic modeling of chloritoid–glaucophane schists from the NW Iberian Massif. *Gondwana Research*, **17**, 377–391.

Martínez Catalán, J.R., Arenas, R., Díaz García, F., Rubio Pascual, F.J., Abati, J. & Marquínez, J. 1996. Variscan exhumation of a subducted Paleozoic continental margin: The basal units of the Ordenes Complex, Galicia, NW Spain. *Tectonics*, **15**, 106–121.

Martínez Catalán, J.R., Arenas, R., Díaz García, F. & Abati, J. 1997. Variscan accretionary complex of northwest Iberia: Terrane correlation and succession of tectonothermal events. *Geology*, **25**, 1103–1106.

Martínez Catalán, J.R., Díaz García, F., Arenas, R., *et al.* 2002. Thrust and detachment systems in the Ordenes Complex (northwestern Spain): Implications for the Variscan–Appalachian geodynamics. *In:* Martínez Catalán, J.R., Hatcher, R.D., Jr, Arenas, R. & Díaz García, F. (eds) *Variscan–Appalachian Dynamics: the Building of the Late Paleozoic Basement*. Geological Society of America, Special Papers, **364**, 163–182.

Martínez Catalán, J.R., Arenas, R., Abati, J., *et al.* 2009. A rootless suture and the loss of the roots of a mountain chain: the Variscan belt of NW Iberia. *Comptes Rendus Géoscience*, **341**, 114–126.

Miller, J.A., Holdsworth, R.E., Buick, I.S. & Hand, M. (eds) 2001. *Continental Reactivation and Reworking*. Geological Society, London, Special Publications, **184**.

Neil, E.A. & Houseman, G.A. 1997. Geodynamics of the Tarim Basin and the Tien Shan in central Asia. *Tectonics*, **16**, 571–584.

Okudaira, T., Takeshita, T., Hara, I. & Ando, J. 1995. A new estimate of the conditions for transition from basal to prism [*c*] slip in naturally deformed quartz. *Tectonophysics*, **250**, 31–46.

Ortega Cuesta, L.A. 1998. *Estudio petrogenético del granito sincinemático de dos micas de A Espenuca (A Coruña)*. Laboratorio Xeolóxico de Laxe, Serie Nova Terra, **14**.

Passchier, C.W. & Trouw, R.A.J. 1996. *Microtectonics*. Springer, Berlin.

Passchier, C.W. & Williams, P.R. 1996. Conflicting shear sense indicators in shear zones; the problem of non-ideal sections. *Journal of Structural Geology*, **18**, 1281–1284.

Pin, C., Paquette, J.L., Santos Zalduegui, J.F. & Gil Ibarguchi, J.I. 2002. Early Devonian supra-subduction zone ophiolite related to incipient collisional processes in the Western Variscan Belt: The Sierra de Careón unit, Ordenes Complex, Galicia. *In:* Martínez Catalán, J.R., Hatcher, R.D., Jr, Arenas, R. & Díaz García, F. (eds) *Variscan–Appalachian Dynamics: the Building of the Late Paleozoic Basement*. Geological Society of America, Special Papers, **364**, 57–71.

Pin, C., Paquette, J.L., Ábalos, B., Santos, F.J. & Gil Ibarguchi, J.I. 2006. Composite origin of an early Variscan transported suture: Ophiolitic units of the Morais Nappe Complex (north Portugal). *Tectonics*, **25**, TC5001.

Ramsay, J.G. & Huber, M.I. 1987. *The Techniques of Modern Structural Geology. Volume 2: Folds and Fractures*. Academic Press, London, 309–700.

Ribeiro, A., Pereira, E. & Dias, R. 1990. Central-Iberian Zone. Allochthonous Sequences. Structure in the Northwest of the Iberian Peninsula. *In:* Dallmeyer, R.D. & Martínez García, E. (eds) *Pre-Mesozoic Geology of Iberia*. Springer, Berlin, 220–236.

Rodríguez, J., Cosca, M.A., Gil Ibarguchi, J.I. & Dallmeyer, R.D. 2003. Strain partitioning and preservation of $^{40}Ar/^{39}Ar$ ages during Variscan exhumation of a subducted crust (Malpica–Tui complex, NW Spain). *Lithos*, **70**, 111–139.

Rodríguez, R., Marcos, A. & Farias, P. 2004. Palynological data on the age of the metasediments of the Parautochthonous Thrust Sheet in the Cabo Ortegal area (Galicia, NW Spain). *Neues Jahrbuch für Geologie und Paläontologie*, **10**, 437–447.

Rodríguez Aller, J. 2005. *Recristalización y deformación de litologías supracorticales sometidas a metamorfismo de alta presión (Complejo de Malpica–Tui, NO del Macizo Ibérico)*. Laboratorio Xeolóxico de Laxe, Nova Terra, **29**.

Röller, K. & Trepmann, C.A. 2003. Stereo32 (v.1.0.1). World Wide Web Address: http://www.ruhr-uni-bochum.de/hardrock/Stereo32.html.

Rubio Pascual, F.J., Arenas, R., Díaz García, F., Martínez Catalán, J.R. & Abati, J. 2002. Eclogites and eclogite–amphibolites from the Santiago Unit (Ordenes Complex, NW Iberian Massif, Spain): a case study of contrasting high-pressure metabasites in a context of crustal subduction. *In:* Martínez Catalán, J.R., Hatcher, R.D., Jr, Arenas, R. & Díaz García, F. (eds) *Variscan–Appalachian Dynamics: the Building of the Late Paleozoic Basement*. Geological Society of America, Special Papers, **364**, 105–124.

Sánchez Martínez, S., Arenas, R., Andonaegui, P., Martínez Catalán, J.R. & Pearce, J.A. 2007*a*. Geochemistry of two associated ophiolites from the Cabo Ortegal complex (Variscan belt of northwest Spain). *In:* Hatcher, R.D., Jr, Carlson, M.P., McBride, J.H. & Martínez Catalán, J.R. (eds) *4-D Framework of Continental Crust*. Geological Society of America, Memoirs, **200**, 445–467.

Sánchez Martínez, S., Arenas, R., Díaz García, F., Martínez Catalán, J.R., Gómez-Barreiro, J. & Pearce, J.A. 2007*b*. Careón Ophiolite, NW Spain: Suprasubduction zone setting for the youngest Rheic Ocean floor. *Geology*, **35**, 53–56.

Santos, J.F., Schärer, U., Gil Ibarguchi, J.I. & Girardeau, J. 2002. Genesis of pyroxenite-rich peridotite at Cabo Ortegal (NW Spain): geochemical and Pb–Sr–Nd isotope data. *Journal of Petrology*, **43**, 17–43.

SCHMID, S.M. & CASEY, M. 1986. Complete fabric analysis of some commonly observed quartz *c*-axis patterns. *In:* HOBBS, B.E. & HEARD, H.C. (eds) *Mineral and Rock Deformation: Laboratory Studies. The Paterson Volume.* American Geophysical Union, Geophysical Monograph, **36**, 263–286.

SIBSON, R.H. 1990. Conditions of fault-valve behaviour. *In:* KNIPE, R.J. & RUTTER, E.H. (eds) *Deformation Mechanisms, Rheology and Tectonics.* Geological Society, London, Special Publications, **54**, 15–28.

SIMPSON, C. & SCHMIDT, S. 1983. An evaluation of criteria to deduce the sense of movement in sheared rocks. *Geological Society of America Bulletin*, **94**, 1281–1288.

TOY, V.G., PRIOR, D.J. & NORRIS, R.J. 2008. Quartz fabrics in the Alpine Fault mylonites: Influence of pre-existing preferred orientations on fabric development during progressive uplift. *Journal of Structural Geology*, **30**, 602–621.

TRÉPIED, L., DOUKHAN, J.C. & PAQUET, J. 1980. Subgrain boundaries in quartz: theoretical analysis and microscopic observations. *Physics and Chemistry of Minerals*, **5**, 201–218.

VALVERDE-VAQUERO, P., MARCOS, A., FARIAS, P. & GALLASTEGUI, G. 2005. U–Pb dating of Ordovician felsic volcanism in the Schistose Domain of the Galicia–Trás-os-Montes Zone near Cabo Ortegal (NW Spain). *Geológica Acta*, **3**, 27–37.

VANDERHAEGE, O. & TEYSSIER, C. 2001. Crustal-scale rheological transitions during late-orogenic collapse. *Tectonophysics*, **335**, 211–228.

VAN ZUUREN, A. 1969. Structural petrology of an area near Santiago de Compostela (NW Spain). *Leidse Geologische Mededelingen*, **45**, 1–71.

WEBB, B.C. & COOPER, A.H. 1988. Slump folds and gravity slide structures in a Lower Paleozoic marginal basin sequence (the Skiddaw Group), NW England. *Journal of Structural Geology*, **10**, 463–472.

WHEELER, J. 1987. The determination of true shear senses from the deflection of passive markers in shear zones. *Journal of the Geological Society, London*, **144**, 73–77.